IOP Publishing Measurement Science and Technology
Meas. Sci. Technol. **25** (2014) 075601 (7pp) doi:10.1088/0957-0233/25/7/075601

Apparatus for temperature-dependent cathodoluminescence characterization of materials

Jan Bok and Petr Schauer

Institute of Scientific Instruments of the ASCR, v.v.i., Kralovopolska 147, 612 64 Brno, Czech Republic

E-mail: bok@isibrno.cz

Received 5 February 2014, revised 14 March 2014
Accepted for publication 28 March 2014
Published 14 May 2014

Abstract

An apparatus for characterization of temperature-dependent cathodoluminescence (CL) of solid-state materials is presented. This device excites a specimen using an electron beam and the CL emission is collected from the specimen side opposite the e-beam irradiation. The design of the temperature-controlled specimen holder that enables cooling down to 100 K and heating up to 500 K is described. The desired specimen temperature is automatically stabilized using a PID controller, which is the proportional-integral-derivative control feedback loop. Moreover, the specimen holder provides *in situ* e-beam current measurement during the specimen excitation. The apparatus allows the measurement of the CL intensity, the CL spectrum, or the CL intensity decay depending on the specimen temperature, or on a variety of excitation conditions, such as excitation energy, electron current (dose), or excitation duration. The apparatus abilities are demonstrated by an example of the CL measurements of the YAG:Ce single-crystal scintillator.

Keywords: cathodoluminescence, electron beam, cryostat, scintillator, YAG:Ce

(Some figures may appear in colour only in the online journal)

1. Introduction

One of the methods for material characterization is photoluminescence using excitation with visible or UV photons, which generate material light emission [1]. Although the photoluminescence is frequently used, it can be inefficient for the characterization of insulators since the photon energy is not sufficient for exciting the material over its band gap. This problem overcomes the material excitation using ionizing particles, whose energy is high enough for the band gap excitation [2]. The special case of the ionizing particles is high-energy electrons. The material excitation with the high-energy electrons can produce cathodoluminescence (CL) emission, whose analysis can be used for characterization and electronic structure study of wide band gap materials [3].

With the development of electron microscopy in the past decades, the sources of high-energy electrons have obtained excellent properties together with good stability and the possibility to change the excitation conditions. Therefore, the high-energy electron excitation has advantages in the frame of the ionizing particle excitation. Modern electron sources have several beneficial features: the electron energy can be changed over many orders from the low electron energies in tens of eV [4] to the high energies in hundreds of keV [5]; the electron current (dose) can be freely changed from single electrons [6] to an electron beam with many electrons having the possibility of forming excitation pulses with variable duration; the e-beam can be focused with the spot diameter in orders of nanometers to excite only the required small volume of the material and, on the contrary, the spot can be expanded in order to decrease the material damage.

Although the electron excitation possesses many benefits, it also has disadvantages. The main drawback is the necessity of positioning the observed specimen into a vacuum chamber because the e-beam is sensitive to the external gas molecules. Luckily, this disadvantage can be turned to a profit when cooling or heating the specimen. The surrounding vacuum decreases the heat flow between the specimen and the specimen

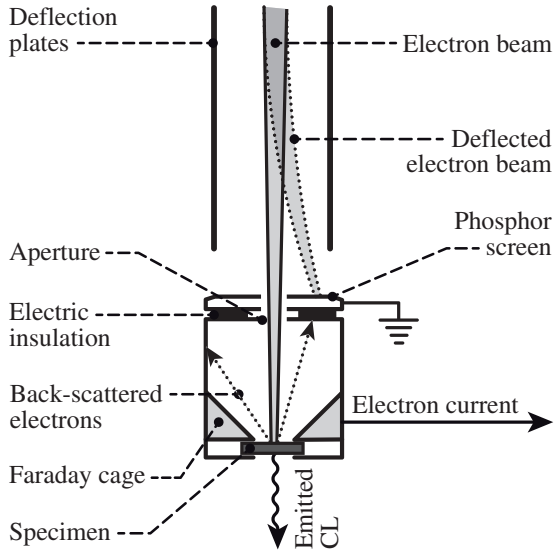

Figure 1. The sectional view at the e-beam excitation assembly. The specimen is excited by the electron beam and the CL emission is collected from the specimen side opposite the e-beam irradiation. The specimen is surrounded by a Faraday cage, which enables measurement of the e-beam current during the specimen excitation. The e-beam can be deflected out of the Faraday cage aperture by an electrostatic deflection system.

chamber and thus the vacuum effectively helps to reach extreme temperatures. Another disadvantage when using the electron excitation is the necessity to coat the specimen surface by a thin conductive layer in order to prevent the surface charging.

An apparatus for the CL material characterization was built in our laboratory in past decades [7, 8]. This device excites a specimen using an electron beam and the CL emission is collected from the specimen side opposite the e-beam irradiation. Although this transmission arrangement suffers from unfavorable influences associated with the passage of the CL emission through the specimen with possibility of re-absorption, or re-excitation processes, there are several reasons for collecting the transmitted CL emission instead of the reflected one. The transmission arrangement gains importance when materials with poor electrical conductivity are characterized, because such materials must be conductively coated for elimination of e-beam charging effects. The coating can totally reflect the CL emission back to the specimen, which makes it impossible to collect the emission at the side of the e-beam irradiation. However, this is an advantage for the transmission arrangement, because the reflection of the coating significantly increases the CL signal. Therefore, the transmission arrangement is preferable when examining optically transparent materials. Moreover, such arrangement usually uses much wider collection angle as compared with the reflection arrangement. This implies higher collection efficiency beneficial in the detection of weak CL signals. Nevertheless, an ideal collection system should offer both alternatives of the CL emission collection. Such a system hasn't been designed in our laboratory yet, but it is planned for future development.

Using the presented apparatus, the measurement of the CL intensity, the CL spectrum, or the CL intensity decay can be carried out, depending on a variety of excitation conditions, such as excitation energy, electron current (dose), or excitation duration. However, former CL measurements weren't able to be performed with specimens cooled below room temperature. The low temperature measurements are important for detailed study of the electronic processes in materials. In this paper, we report the development of a temperature-controlled specimen holder that enables liquid nitrogen cooling down to 100 K and heating up to 500 K. In addition, the specimen holder allows the measurement of the e-beam current during the specimen excitation. Together with the other apparatus abilities, this device provides the possibility for very complex CL measurements. In order to show the apparatus potential in practice, an example of the CL measurements of the YAG:Ce single-crystal scintillator is presented in this paper.

2. Cathodoluminescence apparatus

2.1. Excitation part

The cathodoluminescence (CL) apparatus was built by the reconstruction of the transmission electron microscope Tesla BS-242 into an e-beam source. The specimen holder of the microscope was removed and a new specimen chamber was positioned instead of the chamber designed for image observation and recording. This adapted device emits electrons from a wolfram cathode, which are accelerated and collimated against the specimen surface. The e-beam spot in the specimen plane can have a diameter between 0.1 and 8 mm.

The specimen is surrounded by a cylindrical Faraday cage with an aperture above (see figure 1). The bottom of the Faraday cage holds the specimen and provides an electrical and thermal connection between itself and the specimen. The incident e-beam current (absorbed or reflected by the specimen) is collected by the Faraday cage, which enables the precise measurement of the current during the excitation. The measured current is converted to the voltage and sampled by the Agilent 34401A multimeter. In order to conduct the current from the specimen surface, the specimen must be coated with a thin metal layer. The coating also prevents the material surface from being electrically charged, which can negatively change the CL emission [9].

The e-beam can be deflected out of the Faraday cage aperture by an electrostatic deflection system (figure 1). In order to observe the deflected e-beam spot, an electrically-grounded phosphor screen is positioned above the Faraday cage. The deflected system consists of a pair of deflection plates supplied by the EMG TR-0331 pulse generator with the 25 V voltage amplitude. This solution enables the creation of the e-beam pulses with the variable duration from 50 ns to 50 ms.

2.2. Thermostatic part

The specimen in the Faraday cage can be cooled or heated in the range between 100 and 500 K. For the cooling, the Faraday

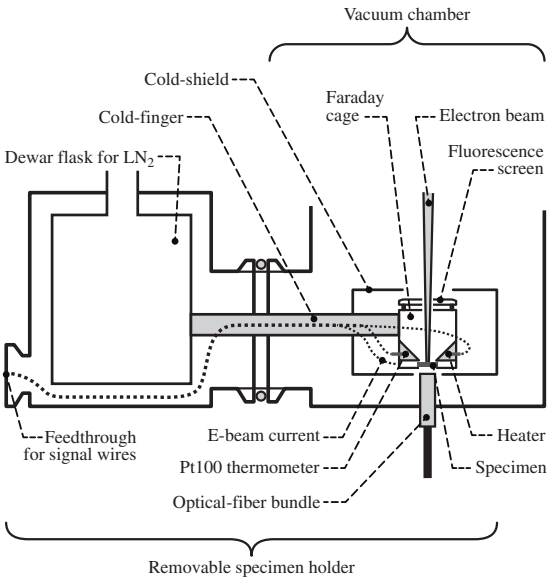

Figure 2. The sectional view at the temperature controlled specimen holder. The Faraday cage with the specimen is held by a cold-finger attached to the liquid nitrogen Dewar flask.

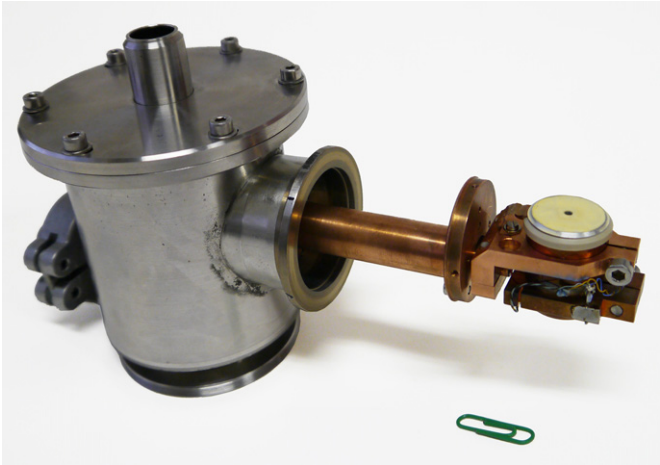

Figure 3. The photograph of the temperature-controlled specimen holder removed from the specimen chamber.

cage with the specimen is held by a tubular copper rod, called a 'cold-finger', attached to a liquid nitrogen Dewar flask with the volume of 118 cm^3 (see figures 2, 3). The Faraday cage must be galvanically insulated from the ground and thus a thin Kapton foil is used as an insulator between the grounded cold-finger and the Faraday cage. The thickness of the foil and its thermal properties are important for the low and high temperature operations of the holder.

When the liquid nitrogen is poured into the Dewar flask, the cold-finger, together with the Faraday cage and with the specimen, is cooled down to at least 100 K. The specimen chamber is under the vacuum pressure of 10^{-2} Pa; thus there is only a low heat flow caused by the residual gas. However, the temperature of the specimen can still be affected by the thermal radiation from the chamber walls, which are at room temperature. In order to shield this radiation, the Faraday cage is surrounded by a cylindrical copper cold-shield mounted directly to the Dewar flask.

The temperature measurement is provided by a Pt100 resistance thermometer and measured by the Agilent 34970A data acquisition unit in the four-wire connection. In order to heat the specimen, the Faraday cage is equipped with a heater consisting of two parallel-connected Pt100 elements that dissipate the heat when supplied by the electric current. The great advantage of using the Pt100 element as a heater is its small size, thermally conductive ceramic package and thermal resilience across a wide range of the temperatures. The disadvantage is the temperature dependency of its electric resistivity and thus of its thermal power. Therefore in our case, the maximum thermal power is 21.9 W at 100 K and only 8.2 W at 500 K when using the Agilent E3632A dc power supply unit with the voltage of 30 V. This disadvantage is particularly eliminated if a control feedback loop is used (see below).

The electrical wires are guided from the vacuum chamber by the vacuum feedthrough located near the Dewar flask. The wires are mechanically fixed (thermally anchored) to the cold-finger. This solution avoids the heat flow through the wires to the specimen during operations with the liquid nitrogen in the Dewar flask. The wires were selected with care in order to provide the thermal stability of its insulation throughout the desired range of temperatures. The Kapton-insulated four-lead bronze wire with the diameter of 0.127 mm is used for the thermometer. The twisted double-lead and single-lead bronze wires are used for the supply of the heater by a current and for the e-beam current measurement, respectively. Both wires have a lead diameter of 0.203 mm and Teflon insulation. All the wires were supplied by Lake Shore Cryotronics, Inc.

For the automatic temperature control, the proportional-integral-derivative control feedback loop, called PID controller, was implemented by a personal computer. The PID controller was programmed in the LabVIEW development environment using the PID and Fuzzy Logic toolkit. The controller acquires the temperature values from the data acquisition unit using GPIB interface and sets the appropriate voltage of the dc power supply unit in order to reach the desired temperature. This enables the stabilization of the specimen temperature in the range of ± 0.5 K. During the thermoluminescence measurements, it is necessary to maintain the linear rate of the heat flow to the specimen. In this case, the tangential slope of the temperature trend is calculated and the PID controller keeps its constant value.

2.3. Detection part

The CL emission is collected from the bottom of the specimen by a silica-glass optical-fiber bundle produced by Optovit, Ltd. The numerical aperture of the optical fibers used is 0.22. The position of the specimen and the optical-fiber bundle is strictly fixed. In order to optimize the signal collection, only the position of the incident e-beam spot can be changed by setting the electron-optical system. The input end of the bundle inside the chamber is vacuum sealed in order to bring the bundle out

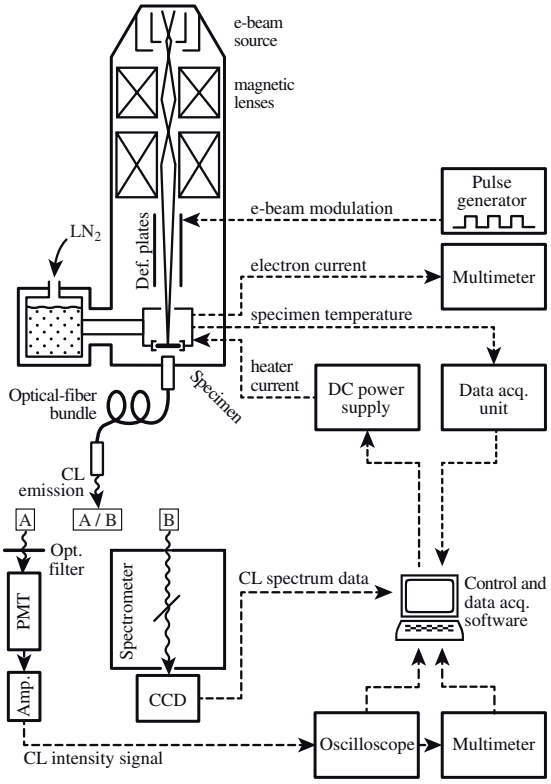

Figure 4. The schematic diagram of the CL measurement set-up. The specimen is excited using the e-beam and the generated CL emission is guided either to the slit of the spectrometer, or to the photomultiplier tube (PMT) equipped optionally by an optical filter.

of the vacuum chamber. The shape of the bundle is different at its opposite sides; the input end has a round shape of 5 mm diameter, while the output end has a rectangular shape with the dimensions of 2 mm $\times$ 10 mm. The rectangular shape at the output end is used for efficient coupling to the entrance slit of a spectrometer.

The output end of the optical-fiber bundle can be coupled either to entrance optics of the spectrometer Horiba JY iHR320 with the Horiba JY Synapse CCD camera, or to the Tesla 65-PK-415 photomultiplier tube (PMT) equipped optionally by an optical filter (figure 4). The spectrometer serves to acquire the CL spectra in the range between 200 and 900 nm with the spectral resolution up to 0.1 nm. The measured spectra are corrected for the apparatus spectral transmittance and for the detector spectral sensitivity using the standard of the spectral irradiance calibrated by the Oriel company.

The electric current from the PMT is amplified and converted to a voltage signal by the Hamamatsu C9663 amplifier. The signal is led either to the Agilent 34401A multimeter to provide the CL intensity measurements, or to the Tektronix DPO7254 oscilloscope to record the CL decay curves. The oscilloscope is synchronized by trigger pulses produced by the pulse generator. All the measurements are controlled by a computer communicating with the individual instruments using the GPIB or USB interface [8].

3. Examples of apparatus application

3.1. Test specimen

The apparatus abilities are demonstrated by the CL measurements of the YAG:Ce single-crystal scintillator [10–12] supplied by CRYTUR, Ltd. The scintillator was grown using the Czochralski method in the ⟨1 1 1⟩ direction with the Ce^{3+} activator concentration of 0.22 mol%. The crystal was cut into the shape of a disc with the diameter of 10 mm and the thickness of 0.5 mm and it was optically polished. Then it was coated with a scandium layer with the thickness of 5 nm to prevent the surface charging.

3.2. Results

The first measurement demonstrates the CL intensity depending on various quantities: on the incident electron energy (figure 5(*a*)), on the electron current (figure 5(*b*)) and on the specimen temperature (figure 5(*c*)). The CL intensity was recorded using the PMT connected to the multimeter. The optical long-pass filter was positioned in front of the PMT in order to detect only the characteristic Ce^{3+} emission in the range between 450 and 800 nm. During all measurements, the specimen was excited by the e-beam with the spot diameter of 2 mm.

The spectral measurement of the CL emission was carried out for different specimen temperatures from 100 to 500 K (figure 6). The desired temperature was set using the PID controller and the temperature was stabilized for approx. 20 min. The specimen was excited by the 10 keV e-beam with the current of 50 nA. The width of the spectrometer entrance slit was set to 1 mm, which enables the recording of spectra with the spectral resolution of 1.8 nm when using a grating with 1800 grooves/mm. The spectra were recorded in the spectral range between 200 and 800 nm. The measured spectra were corrected for the apparatus spectral transmittance and for the detector spectral sensitivity.

The influence of the specimen temperature was also observed in the CL intensity decay. The decay curves for different temperatures recorded after the end of the pulsed excitation are shown in figure 7. The duration of the excitation pulse has influence on the shape of the decay curve. For the demonstration, the duration of 100 ns with the excitation frequency of 2 kHz was chosen. The e-beam energy and the current were set to 10 keV and 50 nA, respectively. The CL intensity was detected in the range between 450 and 800 nm, which is the region of the characteristic Ce^{3+} emission.

Using the electron excitation and the heating of the specimen, the thermoluminescence (TL) can be measured (figure 8). The TL is a form of luminescence that is exhibited by certain materials when the previously absorbed ionizing radiation is re-emitted as light upon the material heating. The specimen was cooled down to 100 K and at this temperature it was irradiated using the 10 keV e-beam with the current of 20 nA for 1 min. Consequently, the specimen was heated with the constant rate of 10 K min^{-1}. The emission in the range between 450 and 800 nm was detected and several TL peaks were registered (figure 8).

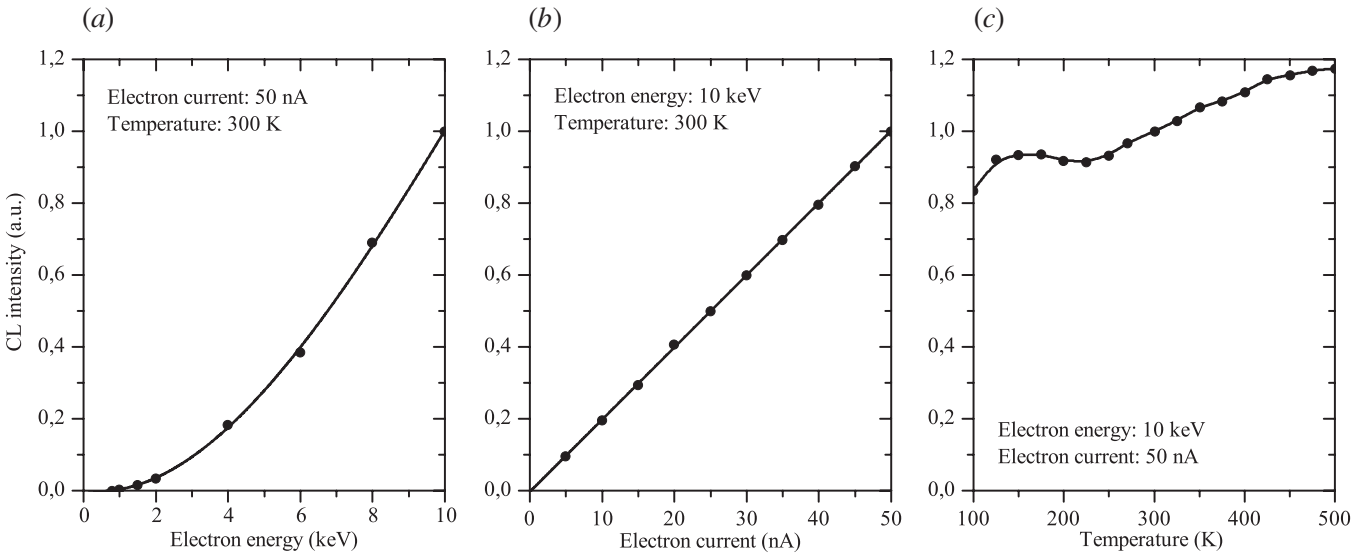

Figure 5. The CL intensity of the YAG:Ce characteristic emission (wavelength range between 450 and 800 nm) as a function of (*a*) the incident electron energy, (*b*) the electron current and (*c*) the specimen temperature.

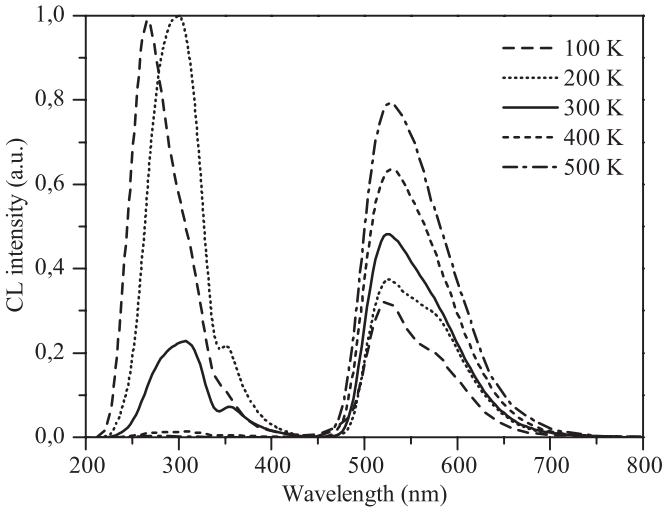

Figure 6. The CL spectrum of the YAG:Ce single-crystal for different specimen temperatures. The specimen was excited by a 10 keV e-beam with a current of 50 nA.

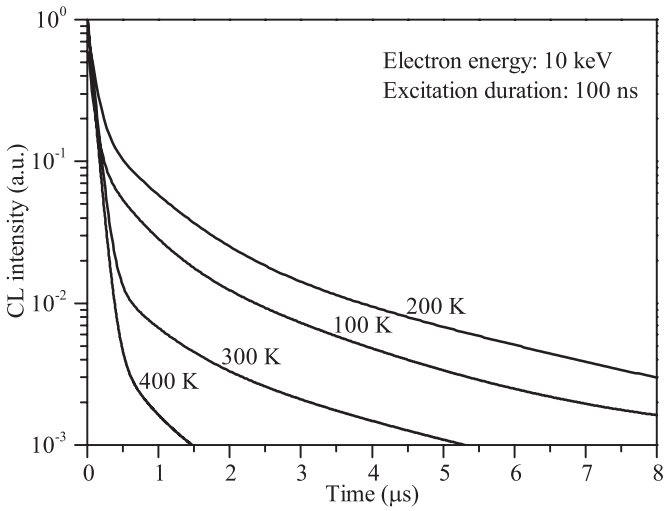

Figure 7. The CL decay of the YAG:Ce characteristic emission (the wavelength range between 450 and 800 nm) for different specimen temperatures. The specimen was excited by a pulsed 10 keV e-beam with a current of 50 nA and with a pulse duration of 100 ns. The excitation frequency of 2 kHz was used.

3.3. Discussion

The CL intensity versus the incident electron energy shows quadratic increase as the energy increases and it becomes linear around the energy of 7 keV (figure 5(*a*)). This behavior results in the electron penetration depth and in the interaction volume as shown in figure 9 created by the Monte Carlo simulation. For the lower energies, the electron penetration is small and a higher portion of the electron energy is dissipated as escaped back-scattered and secondary electrons. But when the electron penetration is higher, the secondary electrons are created deeper below the surface and they have a lower chance to escape from the material. In this case, the incident electrons are effectively converted to the CL emission, and the CL intensity versus electron energy becomes linear. In addition, the dependency of the CL intensity on the electron current shows perfectly linear behavior (figure 5(*b*)). No saturation of the YAG:Ce specimen is observed in the range of the used dose, which is in agreement with [13].

The CL intensity versus specimen temperature shows more complex dependency (figure 5(*c*)). It results in the presence of several temperature-dependent energy transitions, which compete for the excitation energy. Nevertheless, there is the main tendency that the CL intensity increases with the increasing temperature, and the CL intensity begins to be saturated around the temperature of 500 K. The reason for the saturation is the thermal quenching of the YAG:Ce [14]. As the temperature increases, the probability of the non-radiative relaxation rises and the excitation energy is more likely converted into the YAG thermal vibration instead of the radiation emission.

The presented temperature dependency of the CL intensity is supported by the measurement of the CL spectrum

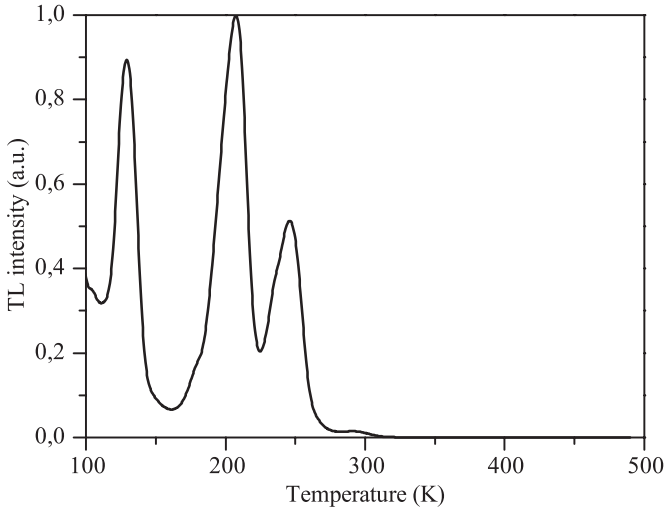

Figure 8. The TL of the YAG:Ce characteristic emission (the wavelength range between 450 and 800 nm). At the temperature of 100 K, the specimen was irradiated using a 10 keV e-beam with a current of 20 nA and then the specimen was heated at a constant rate of 10 K min^{-1}.

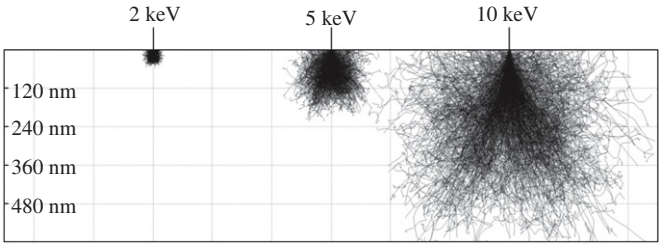

Figure 9. The simulation of the interaction volume of the electrons in the YAG at the 2, 5 and 10 keV electron energies. The simulation was carried out by the Monte Carlo method using the Mott cross-sections.

depending on the specimen temperature (figure 6). The YAG:Ce luminescence spectrum is typical for its characteristic emission band with the center at 550 nm resulting from the Ce^{3+} relaxation [15]. The side band with the center at approx. 300 nm is also presented in the spectrum. This band originates from the radiative transitions of the oxygen vacancies and antisite defects [16]. As the temperature grows, the intensity of this band decreases from high values to almost zero. This can be explained by the thermal ionization of the excited defect states [17, 18]. When the energy level of the excited state is nearly below the conduction band, the excited state can be thermally ionized instead of the radiative relaxation and the released energy can be transferred to other states, such as the Ce^{3+}. Therefore, the intensity of the CL emitted from the defect states decreases with increasing temperature and the CL intensity from the Ce^{3+} increases.

The CL intensity decay obeys complex behavior (figure 7), whose explanation requires more detailed study and is not the subject of this paper. However, the basic tendency of the CL intensity decay is a decrease of the decay time with the increasing temperature. The slow decay is caused mainly by the presence of the meta-stable energy levels (trapping centers) causing the capture of the free charge carriers [19]. Such trapped carriers can be released from the trapping center after some time by the thermal ionization causing the slow CL intensity decay. The growing temperature shortens the mean time for the thermal ionization and thus the decay time decreases.

The existence of the trapping centers is also revealed by the TL measurement (figure 8). At low temperatures, the captured carriers have a very low probability to be released from the trapping centers since sufficient thermal energy wasn't added. With the rising temperature, the probability of the release increases and it is registered as the rise of TL intensity until the carriers are depleted. Therefore, each TL peak represents one type of the trapping center. The position and height of the peak correspond to the activation energy and the abundance of the trapping center, respectively. The activation energy of the trapping center can be calculated from the slope of a single TL peak [20], which is an important parameter for the understanding of the material electronic structure.

4. Conclusion

The material excitation with high-energy electrons has several advantages, such as the possibility of the simple changing of the excitation energy, dose and duration and thus the CL characterization is a useful alternative to the radioluminescence characterization. The CL measurements as a function of the specimen temperature are important for the detailed study of the electronic processes in materials. The presented apparatus for the temperature-dependent CL measurements enables us to reach and stabilize a desired specimen temperature in the range between 100 and 500 K. This device provides the possibility of the complex CL study, such as measurement of the CL intensity, the CL spectra and the CL intensity decays, depending on a variety of conditions. The apparatus abilities were demonstrated on the measurement of the YAG:Ce single-crystal scintillator. Such scintillators are also used as electron–photon convertors in electron microscope detectors [21, 22]. The CL study of scintillators for electron microscopy can reveal their real behavior under high-energy electron excitation [23, 24]. In this case, the CL can be a very reliable and sought-after technique.

Acknowledgments

The authors thank Jiří Sýkora and Tomáš Králík (Institute of Scientific Instruments of the ASCR) for help with the construction of the temperature-controlled specimen holder. The authors also thank the company CRYTUR, Ltd. for the supply of the test specimen. The work was supported by the Technology Agency of the Czech Republic (TE01020118), and by the Czech Science Foundation (14-20012S and 14-22777S).

References

[1] Wright H K and Edwards G V 2008 *Photoluminescence Research Progress* (New York: Nova Science Publishers)
[2] Ronda C R 2008 *Luminescence: From Theory to Applications* (Weinheim: Wiley) pp 1–34

[3] Ozawa L 2010 *Cathodoluminescence and Photoluminescence: Theories and Practical Applications* (Boca Raton, FL: CRC Press)
[4] Erdman N and Bell D C 2012 SEM instrumentation developments for low kV imaging and microanalysis *Low Voltage Electron Microscopy: Principles and Applications* (Chichester: Wiley) pp 31–56
[5] Williams D B and Carter C B 2009 The transmission electron microscope *Transmission Electron Microscopy: A Textbook for Materials Science* (New York: Springer) pp 3–22
[6] Novák L and Müllerová I 2009 Single electron response of the scintillator-light guide-photomultiplier detector *J. Microsc.* **233** 76–83
[7] Horák P and Schauer P 2006 Cathodoluminescence as a method for the study of degradation of polysilanes *Nucl. Instrum. Methods* B **252** 303–7
[8] Bok J and Schauer P 2011 LabVIEW-based control and data acquisition system for cathodoluminescence experiments *Rev. Sci. Instrum.* **82** 113109
[9] Feng X D and Warde C 1993 Influence of surface charge on the cathodoluminescence of Ce:YAG *J. Appl. Phys.* **73** 3926–31
[10] Moszynski M, Ludziejewski T, Wolski D, Klamra W and Norlin L O 1994 Properties of the YAG:Ce scintillator *Nucl. Instrum. Methods* A **345** 461–7
[11] Ludziejewski T, Moszynski M, Kapusta M, Wolski D, Klamra W and Moszynska K 1997 Investigation of some scintillation properties of YAG:Ce crystals *Nucl. Instrum. Methods* A **398** 287–94
[12] Mihokova E *et al* 2007 Luminescence and scintillation properties of YAG:Ce single crystal and optical ceramics *J. Lumin.* **126** 77–80
[13] van der Weg W F and van Tol M W 1981 Saturation effects of cathodoluminescence in rare-earth activated epitaxial $Y_3Al_5O_{12}$ layers *Appl. Phys. Lett.* **38** 705–7
[14] Bachmann V, Ronda C and Meijerink A 2009 Temperature quenching of yellow Ce^{3+} luminescence in YAG:Ce *Chem. Mater.* **21** 2077–84
[15] Wong C M, Rotman S R and Warde C 1984 Optical studies of cerium doped yttrium aluminum garnet single crystals *Appl. Phys. Lett.* **44** 1038–40
[16] Zorenko Y, Voloshinovskii A, Konstankevych I, Kolobanov V, Mikhailin V and Spassky D 2004 Luminescence of excitons and antisite defects in the phosphors based on garnet compounds *Radiat. Meas.* **38** 677–80
[17] Zych E, Brecher C and Glodo J 2000 Kinetics of cerium emission in a YAG:Ce single crystal: the role of traps *J. Phys.: Condens. Matter.* **12** 1947–58
[18] van der Kolk E, Dorenbos P, van Eijk C W E, Basun S A, Imbusch G F and Yen W M 2005 5d electron delocalization of Ce^{3+} and Pr^{3+} in Y_2SiO_5 and Lu_2SiO_5 *Phys. Rev.* B **71** 165120
[19] Nikl M *et al* 2008 Scintillator materials—achievements, opportunities, and puzzles *IEEE Trans. Nucl. Sci.* **55** 1035–41
[20] Varney C R, Mackay D T, Pratt A, Reda S M and Selim F A 2012 Energy levels of exciton traps in yttrium aluminum garnet single crystals *J. Appl. Phys.* **111** 063505
[21] Schauer P and Autrata R 1992 Light transport in single-crystal scintillation detectors in SEM *Scanning* **14** 325–33
[22] Schauer P 2011 Optimization of decay kinetics of YAG:Ce single crystal scintillators for S(T)EM electron detectors *Nucl. Instrum. Methods* B **269** 2572–7
[23] Hibino M, Irie K, Autrata R and Schauer P 1992 Characteristics of YAG single crystals for electron scintillators of STEM *J. Electron. Microsc.* **41** 453–7
[24] Yamamoto K, Tanji T, Hibino M, Schauer P and Autrata R 2000 Improvement of light collection efficiency of lens-coupled YAG screen TV system for a high-voltage electron microscope *Microsc. Res. Tech.* **49** 596–604